RSC Advances

PAPER

View Article Online
View Journal | View Issue

Cite this: *RSC Adv.*, 2026, **16**, 8971

Development of a sensor for the selective detection of manganese in aqueous media using grapefruit peel pectin-decorated silver nanoparticles

Khoa Anh Ton,†[ac] Khang Nguyen-Duy Dao,†[b] Hoa Son Pham,[a] Chi Thi-Kim Huynh,[a] Thu Thi-Cam Nguyen,[a] Phuc Hoang Nguyen,[a] Ty Minh Nguyen[a] and Dung Thi-Kim Hoang *[a]

The presence of Mn^{2+} in aquatic systems even at trace ppm concentrations poses safety concerns; thus, it is indispensable to develop an accurate, sensitive, and selective sensor for Mn^{2+} detection. The use of colorimetric plasmonic nanoparticles offers a suitable approach. Herein, silver nanoparticles were synthesized using pectin (AgGPe NPs), in which the inputs of pectin and $AgNO_3$ and the volume of NaOH were optimized in the reaction to obtain NPs within a size range of 5–45 nm and a zeta potential of −34.26 mV, which were stable for up to 2.5 months at 4 °C. AgGPe NPs were characterized by UV-vis analysis, which revealed a surface plasmon resonance (SPR) peak at 405 nm, along with FTIR and XRD measurements. The formed silver nanoparticles showed specific recognition to Mn^{2+} ions by changing the color from yellow to brown, and the sensing performance was optimized in terms of the input volume of AgGPe NPs, incubation time and pH. The nanocomposite gave a limit of detection (LOD) of 0.5065 ppm, accompanied by a practicable detection for drinking water and Tau Hu canal water with good recoveries. In conclusion, the green-synthesized AgGPe NPs offer a cost-effective and environmentally friendly approach for Mn^{2+} detection and have good prospects for future applications.

Received 13th November 2025
Accepted 1st February 2026

DOI: 10.1039/d5ra08769d

rsc.li/rsc-advances

1. Introduction

Approximately 90% of global manganese production is utilized in the steel industry, primarily as an alloying element to improve strength and hardness.[1] Although manganese is one of the abundant natural metals in the Earth's crust, it enters the living environment through human activities or natural calamities, and it is recognized as a toxic release inventory chemical and as an air contaminant by the Occupational Safety and Health Administration (OSHA). Various heavy metals, such as Cd^{2+}, Cu^{2+}, Hg^{2+}, Mn^{2+}, and Pb^{2+}, are potentially toxic to soil and aquatic organisms, animals, plants, and humans at trace ppm concentrations.[2] In our body, trace elements such as manganese play an important role as cofactors of many cellular enzymes; manganese activates enzymes such as kinases, hydrolases, decarboxylases, phosphatases, peptidases, and transferases.[3] The human intake of manganese is in the range of 2 to 9 mg day^{-1} for a 70 kg individual;[1] however, excess manganese intake has a negative impact on human health because it accumulates in the brain, where it can cause neurotoxicity.[4] Therefore, methods to detect the presence of Mn^{2+} are required to prevent its adverse effects. Conventionally, several methods have been dedicated to detect and measure the presence of manganese ions in water, such as atomic absorption spectroscopy (AAS), inductively coupled plasma mass spectroscopy (ICP-MS), and inductively coupled plasma atomic emission (ICP-AES). These methods require sophisticated equipment, time-consuming preparation, and skilled operators. Another approach that is highly promising for the selective, sensitive, accurate, reliable, and fast detection of manganese ions is nanomaterial-based detection, which is based on the change in the physico-chemical properties in the presence of heavy metals.

To obtain nanoparticles with dimensions between 1 and 100 nm, chemical reduction is of interest, although there remain concerns about the future green development for health and the environment. Biosynthesis, using plants and microorganisms, is an alternative to chemical reduction because it offers a single-step reaction that does not use toxic chemical reagents. It utilizes functional bioactives as reductant and stabilizer; therefore, the biological methods are low-cost and high-yielding, and afford metallic nanoparticles with various sizes, depending on the nature of plant extracts, pH, temperature, concentration, and so on.[5]

In recent years, the use of silver nanoparticles as a means of detection has evolved owing to their optical surface plasmon

[a]*Institute of Advanced Technology, Vietnam Academy of Science and Technology, Vietnam. E-mail: hoangthikimdung@gmail.com*
[b]*Ho Chi Minh University of Technology-Vietnam National University, Vietnam*
[c]*Mekong University, Vinh Long province, Vietnam*
† Equal contributions.

resonance (SPR) properties, wherein a noticeable color change can be induced by local changes that cause a shift in the SPR band.[3] Normally, this SPR is affected by the size and shape of the resultant silver nanoparticles, inter-particle distance, uniformity, the dielectric constant of the medium, and surface functional groups.[4,6,7]

The functional groups and surface ligands present on AgGPe NPs exhibit high affinity toward Mn^{2+} ions, enabling selective binding. This interaction minimizes interference from other competing metal ions and thereby enhances the accuracy of manganese detection.

A research group has used the alginate-stabilized silver nanoparticles for the detection of manganese(II) ions, in which they identified that the cross-linking aggregation of silver nanoparticles in the presence of Mn^{2+}, owing to the decrease in surface charge, was the main mechanism.[4] Another group synthesized silver nanoparticles using *Okara* extract to detect manganese ions in water, with a limit of detection and limit of quantification of 0.01 and 0.03 ppm.[8] Another green synthesis of silver nanoparticles using the extract from *Withania somnifera* was applied as a colorimetric sensor for manganese detection. Optimal synthesis was established at pH 11 with stable nanoparticle formation after 1800 min, using 1.0 mL extract and 1.0 mM $AgNO_3$. TEM analysis revealed spherical AgNPs (43–85 nm), and FTIR spectroscopy confirmed the presence of O–H and C=O groups after reduction and stabilization. Mn^{2+} detection was achieved *via* nanoparticle aggregation, producing a visible color change and a 412 nm absorption peak.[3] Moreover, a process was carried out to form L-tyrosine-capped silver nanoparticles to detect Hg^{2+} and Mn^{2+} in aqueous medium; the limit of detection was 16 nM for both ions under the optimized conditions.[9]

Additionally, lignin-functionalized silver nanoparticles were created by the microwave method to detect Co^{2+}, Cr^{3+}, and Mn^{2+} in aqueous solution. These metal ions caused an aggregation of silver nanoparticles, resulting in the modification of the SPR band, which was characterized by UV-vis. Lignin-decorated silver nanoparticles showed a significant enhancement in the Raman signal for only Mn^{2+}, leading to a selectivity for this ion.[7] Pectin-decorated silver nanoparticles have been employed to recognize a wide range of metal ions in aqueous medium. The process used microwave and commercial pectin. In the presence of Fe^{2+} or Mn^{2+}, they impart black and brown colors, respectively, to the water samples, while Cr^{3+} and As^{5+} induce a reddish brown color.[10] However, there is a need for interference analysis to evaluate the potential practical application of the probe.

In addition to gold nanoparticles, 3-(4-hydroxy-3-methoxyphenyl)-2,3-dihydropyrazolo[3,4-*b*]indole-1(4*H*)-carbothioamide-modified gold nanoparticles were proposed to detect the introduction of Mn^{2+} to environmental water. In this study, a color change from red to blue was observed, and a decrease in the surface plasmon absorption intensity at 520 nm resulted in the formation of a second peak at 655 nm. Additionally, the promoted probe exhibited a limit of detection of 0.00233 mg L^{-1} with a linear range of 0.5–10 mg mL^{-1}, with a good sensitivity towards Mn^{2+} without being selective to other anions and cations.[11]

In this research, as depicted in Scheme 1, we have developed a green pathway for silver nanoparticle synthesis using grapefruit pectin (AgGPe NPs) and a method for manganese(II) ions (Mn^{2+}) detection in water. Pectin is a natural polysaccharide in the plant cell wall, which is cheap, biodegradable, and non-toxic.[12] In an alkaline medium, the hydroxyl groups are converted into aldehyde groups, which reduce the metal salts into metallic nanoparticles. First, grapefruit pectin (GPe) was used to convert silver ions into silver nanoparticles in an alkaline medium; the nanoparticles were characterized by UV-vis analysis, focusing on the SPR shifts, FTIR, XRD, and TEM. Herein, the weight of the grapefruit pectin, the concentration of $AgNO_3$, and the volume of 1 M NaOH were the parameters for assessing the optimal conditions. Second, the performance of the AgGPe NP sensor to manganese ions (Mn^{2+}) was investigated by measuring the linear increase in absorption intensity of A_{525}/A_{405} and determining the correlation coefficient (R^2). This nanosensor can be applied for selective Mn^{2+} detection that

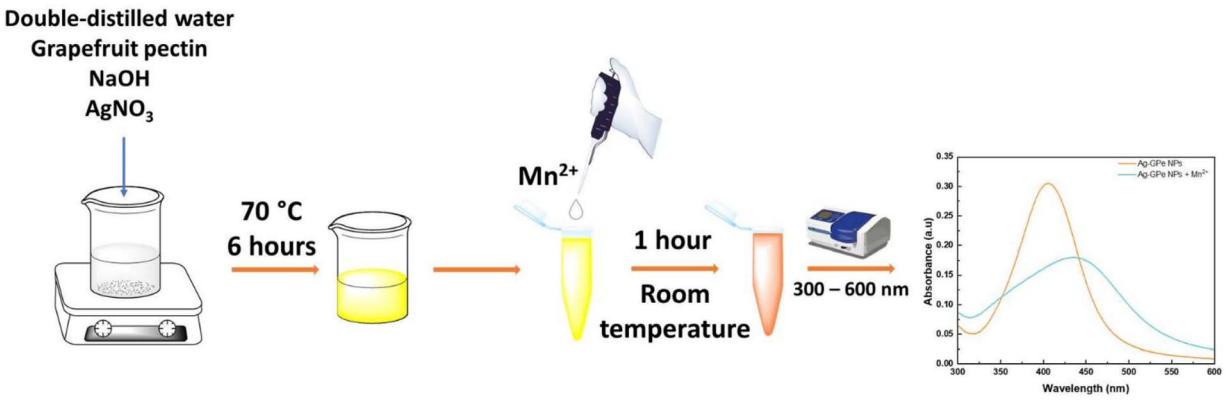

Scheme 1 Grapefruit pectin-decorated silver nanoparticles were synthesized and subsequently applied for the detection of manganese ions in aqueous medium. The preparation procedure involved mixing double-distilled water, pectin, silver nitrate and sodium hydroxide, followed by heating at 70 °C for six hours. This process yielded a yellow dispersion of silver nanoparticles. An aliquot of the dispersion was then utilized for manganese ion sensing, where the appearance of a brown color after one hour indicated the presence of manganese ions.

satisfies the basic conditions of selectivity, sensitivity, accuracy, and ease of use.

2. Methodology

2.1. Materials

Silver nitrate ($AgNO_3$) was a product of Merck (purity 99%), sodium hydroxide (NaOH) was purchased from Fischer (purity 97%), and hydrochloric acid was from Xilong Scientific Co., Ltd, China. The metal ions nickel(II) chloride hexahydrate ($NiCl_2 \cdot 6H_2O$); cadmium(II) chloride monohydrate ($CdCl_2 \cdot H_2O$); chromium(III) chloride hexahydrate ($CrCl_3 \cdot 6H_2O$); copper(II) chloride dihydrate ($CuCl_2 \cdot 2H_2O$); aluminum chloride hexahydrate ($AlCl_3 \cdot 6H_2O$); manganese(II) chloride tetrahydrate ($MnCl_2 \cdot 4H_2O$); Iron(III) nitrate nonahydrate ($Fe(NO_3)_3 \cdot 9H_2O$); zinc chloride ($ZnCl_2$); cobalt(II) chloride hexahydrate ($CoCl_2 \cdot 6H_2O$); and lead(II) acetate ($Pb(OOCCH_3)_2$) were used to prepared solutions of 1000 ppm.

Tri-sodium phosphate dodecahydrate ($Na_3PO_4 \cdot 12H_2O$), sodium sulfate anhydrous (Na_2SO_4), sodium thiosulfate pentahydrate ($Na_2S_2O_3 \cdot 5H_2O$), di-sodium tetraborate decahydrate ($Na_2B_4O_7 \cdot 10H_2O$), sodium acetate anhydrous (CH_3COONa), tri-sodium citrate dihydrate ($Na_3C_6H_5O_7 \cdot 2H_2O$), urea ($CO(NH_2)_2$), and sodium thiocyanate (NaSCN) were purchased from Xilong Scientific Co., Ltd (China) and used as anionic interferes at a concentration of 1000 ppm.

Double-distilled water (DD water) was prepared at the Department of Organic and Environmental Technology, Ho Chi Minh City Institute of Advanced Technology (IAT), Vietnam Academy of Science and Technology (VAST). Grapefruit pectin was isolated and purified at the Department of Organic and Environmental Technology, IAT-VAST, as we have published previously.[13]

2.2. Preparation of silver nanoparticles from grapefruit pectin

The synthesis of silver nanoparticles (AgGPe NPs) was carried out using pectin extracted from grapefruit peel (GPe). Initially, 15.8 mL of DD water was heated to 70 °C. Subsequently, 10.0 mg of GPe was added, and the mixture was stirred until a clear solution was obtained. Then, 300 μL of $AgNO_3$ 10 mM was added dropwise to the obtained solution. After 5 minutes, 100 μL of 1 M NaOH was added, and the reaction was allowed to proceed for 6 hours, yielding a yellow solution of AgGPe NPs. The resulting solution was stored at 4 °C for Mn^{2+} detection. The solution was lyophilized to obtain the powder form for physicochemical characterization (if necessary).

2.3. Characterization

UV-vis spectroscopy was employed to investigate the green synthesis of silver nanoparticles by monitoring the intensity and position of the SPR signals. Herein, 500 μL of AgGPe NPs was diluted to 2 mL with DD water, and the absorbance was measured at 300–600 nm with 1 nm resolution with a Jasco V-770 UV-vis spectrophotometer. Next, a volume of 40 μL of AgGPe NPs was diluted 100-fold with DD water to determine particle size and zeta potential at 25 °C, using a Horiba SZ-100 instrument. Fourier-transform infrared spectroscopy (FTIR) was conducted to identify the potential functional groups involved in the reduction and stabilization of the nanoparticles by pectin. For FTIR analysis of the GPe and AgGPe NPs, the sample was mixed with KBr, pressed into a pellet, and scanned using an FTIR spectrometer (Bruker Tensor 27, Germany) in the 4000–500 cm^{-1} wavenumber range. X-ray diffraction (XRD) analysis was performed to evaluate the crystalline structure and phase purity, using a drop-coated film method on a glass substrate, scanned over a range of 10–80° at room temperature.[14] Finally, high-resolution transmission electron microscopy (HR-TEM) was used to capture the morphology of AgGPe NPs, wherein 100 random nanoparticles were picked to establish the size distribution.

2.4. Selectivity of the sensor

Selectivity means that only the target analyte is detected and the measurement is not easily disturbed by impurities.[15] To evaluate the selectivity of the sensor, 0.5 mL of silver nanoparticles (AgGPe NPs) was mixed with 100 μL of various metal ions (Ni^{2+}, Cr^{3+}, Cd^{2+}, Cu^{2+}, Zn^{2+}, Co^{2+}, Pb^{2+}, Al^{3+}, Fe^{3+}, and Mn^{2+}) at a concentration of 10 ppm. The mixture was then adjusted to a final volume of 2 mL with DD water using a vortex to ensure homogenization. The reaction mixture was allowed to stand for 2 hours, after which absorbance was measured with a UV-vis spectrophotometer.

Additionally, ethylenediaminetetraacetic acid (EDTA) was used to determine the interaction between AgGPe NPs and Mn^{2+}. The experiment was designed following the correct order of reagent addition, as illustrated in Scheme 2.

Initially, 0.5 mL of AgGPe NPs and sufficient volumes of DD water were added to three test tubes, designated as 1, 2, and 3 (AgGPe NPs blank sample, AgGPe-Mn^{2+} complex, and AgGPe-EDTA-Mn^{2+} mixture, respectively). In tube 3, 0.1 mL of EDTA 50 mM was introduced and vortexed for 10 seconds. Subsequently, 0.1 mL of Mn^{2+} 50 ppm was added to tubes 2 and 3. The total volume in each tube was adjusted to 2 mL. After 1 hour, the absorption spectra were recorded using a spectrophotometer, along with color observation with the naked eye.

2.5. Sensitivity of the sensor

Solutions containing manganese ions with concentrations ranging from 0.1 to 50 ppm were prepared. An aliquot of 0.1 mL of the Mn^{2+} solution was added to 0.5 mL of the silver nanoparticle (AgGPe NPs) suspension, followed by the addition of 1.4 mL of DD water to obtain a total reaction volume of 2.0 mL. The mixture was homogenized using vortexing and subsequently allowed to stand at room temperature for 2 hours to facilitate the interaction between Mn^{2+} ions and AgGPe NPs. After incubation, the optical properties of the resulting solution were analyzed using a UV-vis spectrophotometer to monitor changes in absorbance associated with nanoparticle surface plasmon resonance.

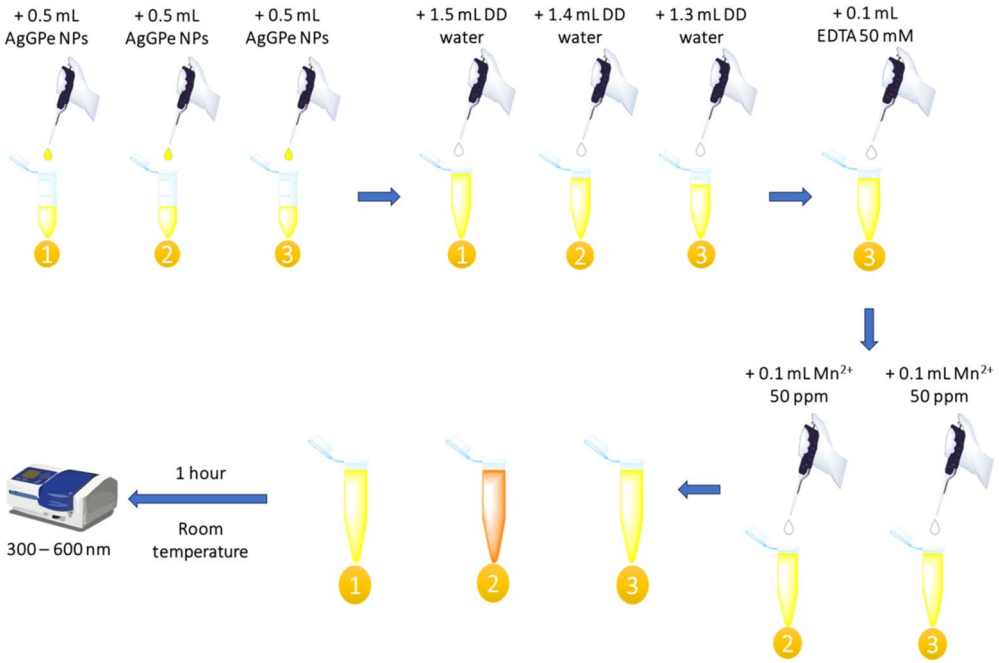

Scheme 2 Experimental design for determining the interaction between nanoparticles and the analyte with and without EDTA.

2.6. Optimization of detection

The sensing conditions were optimized to define suitable incubation time, volume of AgGPe NPs, and pH for the colorimetric observation strategy.

Regarding the volume of AgGPe NPs, 0.3 or 0.5 mL of AgGPe NPs was added with water and 0.1 mL of Mn^{2+} with a concentration in the range 0–50 ppm to reach a uniform 2 mL mixture. These solutions were left for 120 min. The standard for comparison was composed of AgGPe NPs and water.

For the incubation time, 0.5 mL of AgGPe nanoparticles (NPs) was diluted with 1.4 mL of DD water. Subsequently, 0.1 mL of Mn^{2+} solution at varying concentrations (0–50 ppm) was added to achieve a final homogeneous volume of 2.0 mL. The prepared mixtures were incubated for different time intervals: 0.5, 1, 3, 5, 10, 30, 60, and 120 minutes. A control sample was composed of AgGPe NPs diluted only with DD water (without Mn^{2+}) and used as the standard.

Environmental pH: To simulate realistic environmental conditions, the stability of the AgGPe nanoparticles (NPs) was evaluated across a range of pH values. The initial post-synthesis pH of AgGPe NPs was 11.36, which was subsequently adjusted to target values (pH 3, 5, 7, 9, and 11.36) using 1 M HCl or 1 M NaOH. For stability assessment, 0.5 mL of AgGPe NP solution at each pH was diluted with 1.5 mL of double-distilled water and incubated for 60 minutes. The absorbance spectra were then recorded at 405 nm to determine the influence of pH on nanoparticle stability.

For evaluation of optimal pH conditions for sensing performance, 0.5 mL of AgGPe NP solution (adjusted to the same pH values: 3, 5, 7, 9, and 11.36) was diluted with 1.4 mL of DD water, followed by the addition of 0.1 mL of Mn^{2+} solution (10 ppm) to yield a homogeneous final volume of 2.0 mL. These mixtures were incubated for 1 hour, after which the absorbance ratio (A_{525}/A_{405}) was calculated to identify the most suitable pH conditions for sensing applications.

The limit of detection (LOD) of the promoted sensor AgGPe NPs was calculated as follows:[16–18]

$$\mathrm{LOD} = 3 \times \frac{\mathrm{SD}}{\mathrm{Slope}} \quad (1)$$

$$\mathrm{SD} = \mathrm{SE} \times \sqrt{n} \quad (2)$$

Here, LOD: limit of detection, SD: standard deviation of the response, SE: standard error of the intercept, n: sample size ($n = 12$).

2.7. Effect of interferences

The sensor (0.5 mL) was diluted with 1.3 mL of DD water. Subsequently, 0.1 mL of competitors (Al^{3+}, Cd^{2+}, Co^{2+}, Cr^{3+}, Cu^{2+}, Fe^{3+}, Ni^{2+}, Pb^{2+}, Zn^{2+}, and anions), each prepared at a concentration of 10 ppm, was added to the mixture. Following this, 0.1 mL of Mn^{2+} solution (also 10 ppm) was introduced to obtain homogeneous mixtures.

AgGPe NPs alone and AgGPe-Mn^{2+} were employed as reference samples. After incubating for 1 hour at room temperature, the optical responses of all mixtures were recorded using UV-vis spectroscopy. The absorbance data were subsequently processed to construct a comparative bar chart, illustrating the sensor's response to Mn^{2+} in the presence of various competing ions.

2.8. Real water test

Three samples were collected from drinking water, laboratory tap water, and the Tau Hu canal. They were centrifuged and filtered through a 0.22 μm PTFE membrane to remove dust and solid residues. The treated samples were then used to prepare

Mn^{2+} stock solutions at a concentration of 1000 ppm, which were further diluted to working solutions of 1 ppm, 5 ppm, and 10 ppm.

The procedure for sensing Mn^{2+} was as follows: 0.5 mL AgGPe NPs was diluted with 1.4 mL DD water. To this solution, 0.1 mL Mn^{2+} solution at concentrations of 1 ppm, 5 ppm, or 10 ppm was added. The final volume of 2.0 mL was homogenized using a vortex and incubated at room temperature for 1 hour.

The absorbances were recorded by UV-vis spectroscopy. Mn^{2+} concentrations were quantified based on the linear calibration equation, and recovery percentages were calculated to evaluate the accuracy of the sensor in real water matrices.

2.9. Statistical analysis

All tests were conducted in triplicate, and the results are presented as mean ± SD.

3. Result and discussion

3.1. Optimization of silver nanoparticle formation using grapefruit pectin (AgGPe NPs)

In the present study, silver nanoparticles (AgGPe NPs) were successfully synthesized *via* a green, rapid one-pot method, employing grapefruit pectin (GPe) as both a reducing and stabilizing agent. Understanding the formation of AgGPe NPs requires careful consideration of critical parameters, including the concentration of pectin, silver nitrate ($AgNO_3$), and the reaction pH. These factors can influence the nucleation rate, leading to variations in size, morphology, and polydispersity. In particular, the pH will influence the ionization state, reactivity of reductant, reduction potential of silver ions, as well as the surface charge of the resulting nanoparticles.[3,19,20] These parameters need to be controlled to ensure a suitable size, shape, and stability for practical applications.

Pectin was recovered from pomelo peel, as described in our previous research at the Department of Organic and Environmental Technology, Ho Chi Minh City Institute of Advanced Technology (IAT), Vietnam Academy of Science and Technology (VAST). It has a molecular weight of 399 498–1 881 678 kDa, and an esterification degree of 34.2%. Its monosaccharide composition is summarized in Table 1.[13]

Table 1 Monosaccharide composition of pectin

Name	Composition (%)
Mannose	3.6
Ribose	0.3
Rhamnose	4.5
Glucuronic acid	32.1
Galacturonic acid	7.0
Glucose	7.5
Xylose	22.4
Galactose	3.3
Arabinose	18.3
Fucose	0.9

The formation of AgGPe NPs was visually confirmed by a distinct color change from colorless to yellow or dark brown under alkaline conditions. These color changes are characteristic of localized surface plasmon resonance (LSPR), which originates from the collective oscillation of conduction electrons on the nanoparticle surface upon interaction with incident light.[7,14] To evaluate the formation of silver nanoparticles mediated by GPe, UV-vis spectroscopy was carried out to define the position and intensity of the surface plasmon resonance peak. As shown in Fig. 1A, varying the GPE input (5–15 mg) significantly influenced the spectral response. Specifically, 10 mg of GPe gave the highest absorbance peak at 405 nm, without any secondary signal in the range of 500–525 nm. Using less than 10 mg of reductant, for instance, 5 and 7.5 mg, would promote SPR peaks with lower intensity, along with a secondary peak at 525 nm. We increased the GPe as well as increased the number of functional groups to convert the silver ions into silver nanoparticles.[21]

Secondly, the concentration of $AgNO_3$ also influences the morphology of the formed nanoparticles, as shown in Fig. 1B. We observed that the higher the concentration of silver substrate, the more intense the SPR peak. However, beyond 300 μL of $AgNO_3$ 10 mM, the SPR peaks were still located at 405 nm

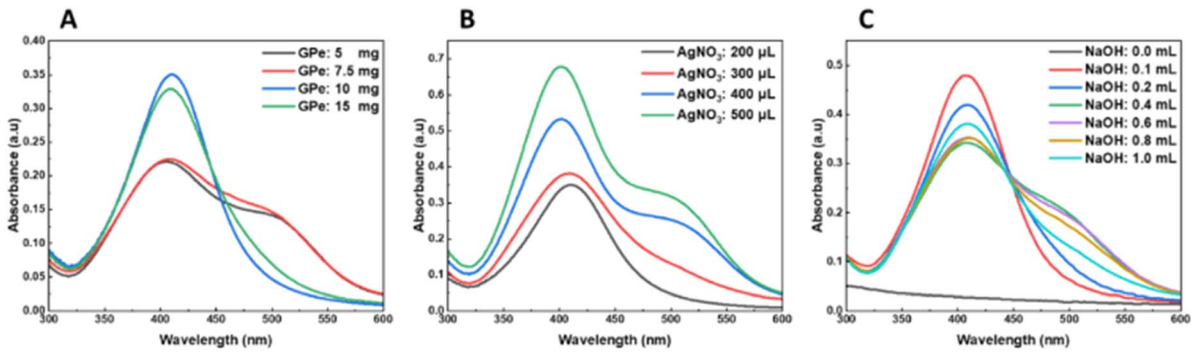

Fig. 1 UV-vis spectra of grapefruit pectin-decorated silver nanoparticles (AgGPe NPs) recorded to evaluate the synthesis process. The spectra highlight the influence of three key parameters on nanoparticle formation: (A) amount of pectin, (B) concentration of silver nitrate ($AgNO_3$), and (C) volume of 1 M sodium hydroxide (NaOH).

with secondary peaks in the range 500–525 nm. Increasing $AgNO_3$ concentration led to the formation of more nanoparticles, but it showed a tendency to produce larger particles and even aggregation when excessive substrate was used.

Finally, Fig. 1C shows the impact of the volume of 1 M NaOH on the formation of silver nanoparticles. In the absence of NaOH (pH 5.5), no nanoparticles were observed. In contrast, the addition of 100 μL of 1 M NaOH (pH 11.36) produced the highest absorbance at the SPR peak, which subsequently decreased as the pH increased further. Thus, the acidic pH inhibited the reaction due to the high net positive charge of the solution,[21] whereas alkaline conditions favored this process owing to the formation of aldehyde groups, which are specified for the reducing nature of pectin.[12] The mechanism to produce silver nanoparticles by pectin is noteworthy, and it relies on the formation of the reducing sugar galactose, along with a non-reducing sugar, galacturonic acid, as pectin is hydrolyzed at high temperatures in alkaline media. Galactose undergoes a series of reactions, such as dehydration, decomposition, polymerization, condensation, and aromatization to form C-dots, which have significant reducing power owing to their lower reduction potential than that of silver ions, favoring the reduction of Ag^+ to Ag, which, in turn, is expressed as the maximum surface plasmon resonance at 405 nm.[22] Furthermore, according to our research group's previous report, the isolated pectin material has an esterification degree of approximately 34.2%,[13] implying that the ester hydrolysis process in alkaline medium contributes to the formation of carboxyl ($-COO^-$) groups, providing additional agents that act as reducing agents and stabilizers in the process of forming silver nanoparticles.

Therefore, the parameters fixed for the green synthesis of silver nanoparticles are 15.8 mL of double-distilled water, 10 mg of grapefruit pectin, 300 μL of $AgNO_3$ 10 mM, and 100 μL of 1 M NaOH at a temperature of 70 °C for a reaction time of 6 hours, which forms a yellow solution as the key indicator for the rapid and green process. Compared with some previous reports, our data were similar in some respects. For instance, silver nanoparticles synthesized from *Withania somnifera* extract had a prominent SPR peak at 412 nm, and the TEM measurements showed a size of about 43–85 nm.[3] In other work, by using *Okara* extract, nanosilver was formed that showed the SPR peak at 412 nm, and had a size of approximately 13.4 nm by microscopic analysis.[8]

Understanding the physicochemical properties of AgGPe NPs is crucial for exploring the best conditions for sensor development; thus, we employed some techniques to assess the important characteristics.

The FT-IR spectrum of GPe (Fig. 2A) reveals a prominent peak at 3439 cm^{-1}, showing stretching vibrations of the –OH group. The peak at 2856 cm^{-1} is caused by C–H stretching of methyl esters of galacturonic acids. The absorption peak at 1610 cm^{-1} represents C=O stretching vibrations of ionic carboxyl groups.[23] The signal at 1735 cm^{-1} suggests a carbonyl (C=O) group.[24] The strong band at 1409 cm^{-1} is caused by symmetric stretching vibrations of the carboxylate group.[4] The spectra of AgGPe NPs show a notable shift, indicating a change in functional groups. The carbonyl (C=O) peak (1735 cm^{-1}) shifts to a higher wavelength of 1741 cm^{-1}. The peak for C=O stretching vibrations of the ionic carboxyl groups (1610 cm^{-1}) moves to a lower wavelength of 1602 cm^{-1}. The reason could be that carbonyl groups participate in the reduction of Ag^+ to Ag. The absorption frequencies occur at 3439 cm^{-1}. This band has lost strength, indicating that the hydroxyl groups were involved in the reduction reaction or interacted with the silver nanoparticles. The strength of the $-COO^-$ symmetric stretching vibration at 1411 cm^{-1} rose substantially. Based on these findings, we conclude that GPe's hydroxyl and carboxyl groups contributed significantly to the creation and stability of the silver nanoparticles.

X-ray diffraction is a vital analytical technique to understand the crystallographic structure and phase purity of nanomaterials. The data for AgGPe NPs, presented in Fig. 2B, exhibited the well-defined peaks at 38.18°, 44.27°, 64.38°, and 77.27°, corresponding to the (111), (200), (220), and (311) crystallographic planes, respectively. These planes are in good agreement with the standard face-centered cubic (fcc) crystal structure of metallic silver, and are in line with previous studies.[4,14,25] The highest intensity peak at 38.18° indicates the high crystallinity and well-ordered atomic arrangement at the nanoscale. Likewise, Fig. 2C depicts the stabilization of AgGPe NPs in terms of unchanged intensity and the position of the LSPR peaks, accompanied by the inset of 2 months stabilized silver nanoparticles; thus, grapefruit pectin can protect the formed nanoparticles from aggregation and ensure the extended lifetime of AgGPe NPs.

To examine the general morphology of the nanosilver particles, Fig. 2D presents a TEM image of AgGPe NPs, which reveals the uniformly dispersed spherical nanoparticles with a size in the range of 5–45 nm, with the majority of particles exhibiting a size of 23.4 ± 7.1 nm (presented in Fig. 2E). This indicates efficient nucleation and stabilization by pectin upon synthesis. Hence, it is demonstrated that the formation of silver nanoparticles by grapefruit pectin was successfully achieved by its reducing and stabilizing ability to produce the particles with specified characteristics for sensor development. Our results are comparable to those obtained for silver nanoparticles that were formed by other groups. For instance, K. B. Narayanan *et al.* utilized sodium alginate to generate spherical silver nanoparticles with sizes ranging from 10 to 20 nm.[4] When using plant extracts as reducing and stabilizing agents for nanosystems, M.U. Rahman *et al.* synthesized spherical silver nanoparticles ranging in size from 43 to 65 nm using *Withania somnifera* extract.[3] Furthermore, P. Panjina *et al.* performed studies employing *Okara* extract for creating spherical silver nanoparticles ranging in size between 2 and 50 nm.[8]

3.2. Colorimetric and selective detection of Mn^{2+}

Regarding the selectivity of the sensor, there are many aspects that determine the feasibility of interactions between the probe and analytes, such as the type of surface ligands and nature of the analytes and surrounding environment. In the context of surface ligands, there is a vast amount of research on the

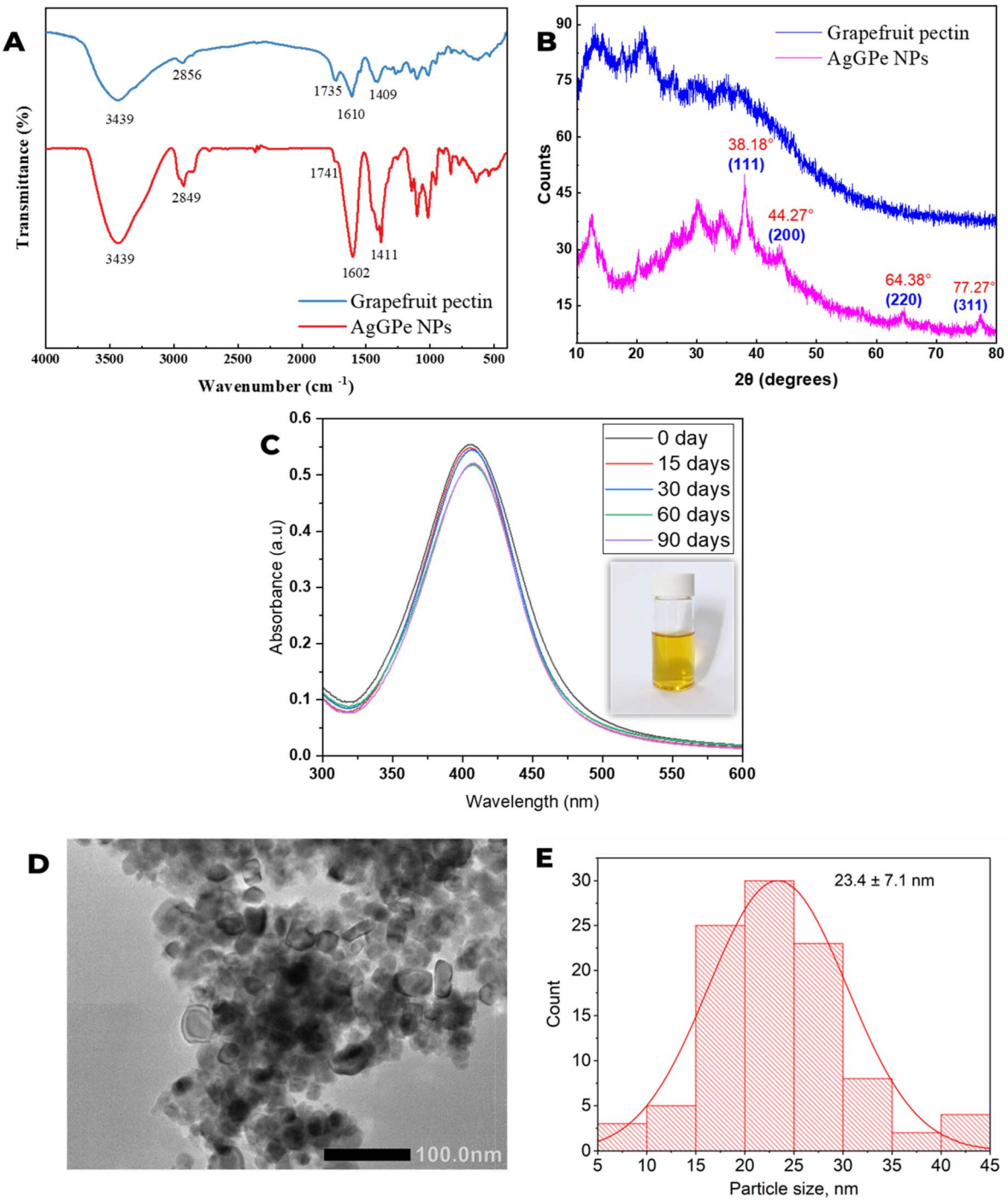

Fig. 2 Comprehensive characterization of grapefruit pectin and grapefruit pectin-decorated silver nanoparticles (AgGPe NPs): (A) FTIR spectra, (B) XRD diffraction patterns, (C) stability profile of AgGPe NPs after 2.5 months with inset showing post-storage colloidal suspension, (D) HR-TEM micrograph of AgGPe NPs, and (E) particle size distribution.

specific organic electron-rich groups that can coordinate with metal ions, such as –SH, $–NH_2$, –OH, and –COOH.[9,26] The structure of pectin contains –OH and –COOH, which are favored for metal binding.

Under the introduction of Mn^{2+}, the SPR peak of silver nanoparticles will change and shift to a longer wavelength, which indicates aggregation of the nanoparticles.[9,26] Therefore, the absorbance intensity ratio was a critical parameter to define the concentration of the analyte. This ratio can vary depending on the relevant physicochemical properties of the silver nanoparticles, such as A_{520}/A_{408} (ref. 9) and A_{550}/A_{408}.[27] In this study, AgGPe NPs showed a significant SPR peak at 405 nm, which was used for detecting various metal ions, and changes in this band will lead to a signal for selective sensing of the relative

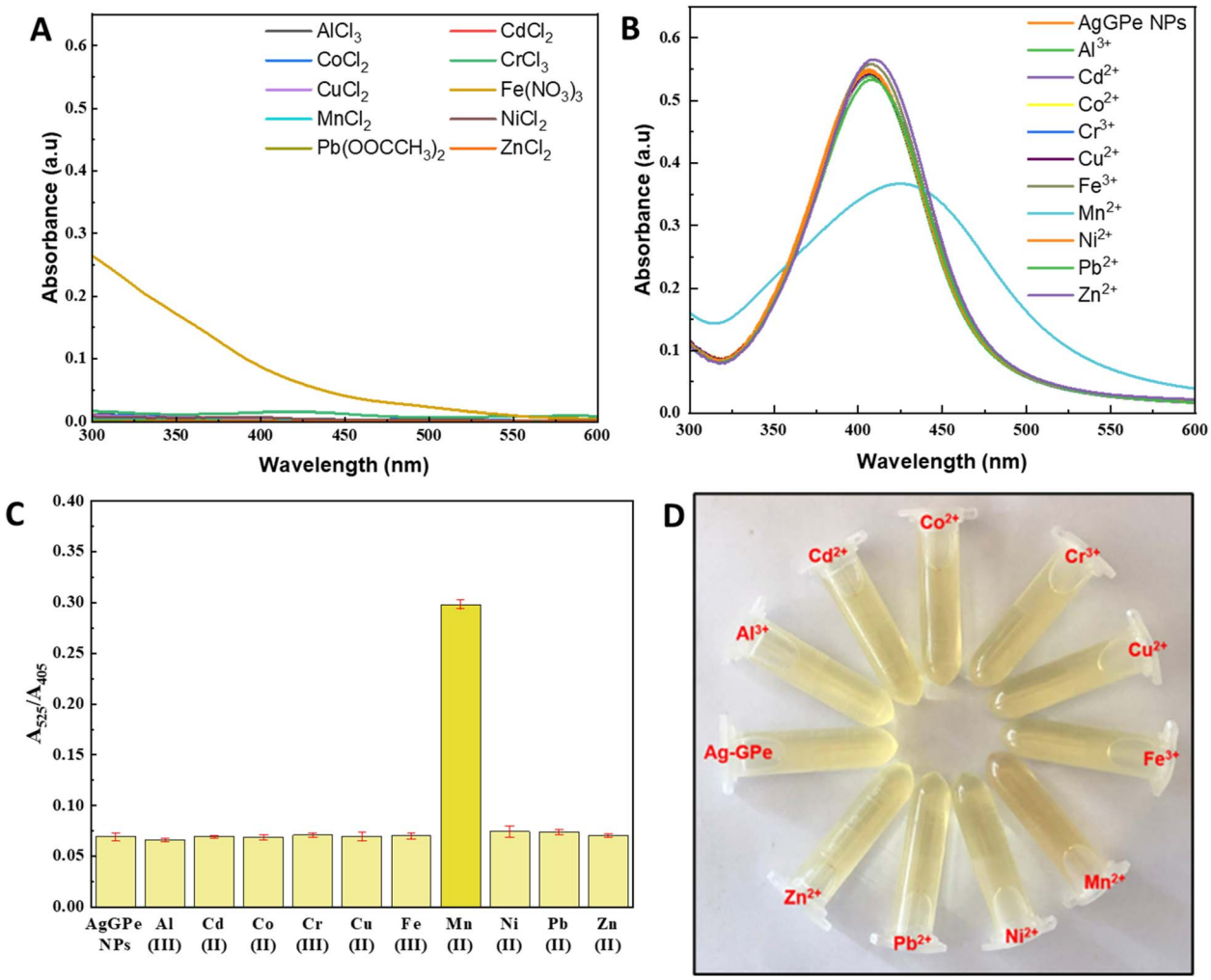

Fig. 3 Spectroscopic and visual evaluation of grapefruit pectin-decorated silver nanoparticles (AgGPe NPs) in the presence of different cations: (A) UV-vis spectra of individual cations, (B) UV-vis spectra of AgGPe NPs following incubation with various cations, (C) bar chart comparing the absorption ratios (A_{525}/A_{405}) of AgGPe NPs before and after incubation, and (D) representative color changes illustrating the selective response of AgGPe NPs toward manganese ions compared with other cations.

contaminant. First, the metal ions in their relative salt solutions exhibited no prominent signals from 300–600 nm, as shown in Fig. 3A. When AgGPe NPs were immersed in a solution containing 10 different metal ions, only Mn^{2+} could lower and shift the SPR peak to a longer wavelength, as shown in Fig. 3B. Regarding Fig. 3C, by building a bar chart of the absorbance ratio of A_{525}/A_{405} towards various metal ions, Mn^{2+} offered the highest bar compared with the other metal ions. Moreover, the naked eyes observation in Fig. 3D illustrates the distinct color change induced by Mn^{2+}, modifying the base color of AgGPe NPs compared to other tested metal ions.

The Mn^{2+} ion sensing mechanism of AgGPe NPs is explained schematically in Scheme 3A. Silver nanoparticles are surrounded by negatively charged groups such as carboxyl or hydroxyl groups (–OH), which allow the silver nanoparticles to separate from one another through the interaction of negatively charged groups. When Mn^{2+} ions are present in an aqueous medium, negatively charged components such as carboxyl ($-COO^{-}$) or hydroxyl groups (–OH) interact with them, causing changes in the grapefruit pectin chain structure. This forces the silver nanoparticles closer together, causing aggregation and a change from yellow to brown color. In 2017, K. B. Narayanan *et al.* used alginate as a reducing agent and stabilizer for the silver nanosystem in the Mn^{2+} ion sensor. The negatively charged components of the alginate polymer chain formed bonds with Mn^{2+} ions, changing the chain's structure and causing silver nanoparticle aggregation.[4]

On the other hand, in 2015, W. Plazinski *et al.* released a study on the topic of complicated ion heavy metal-polyuronates.[28] The authors argued that the interaction of divalent ions and biopolymer anions is a regular occurrence in nature. This procedure, which is similar to biological adsorption, is used in wastewater treatment to remove heavy metal ions such as Cu^{2+}, Cd^{2+}, Co^{2+}, Mn^{2+}, and Zn^{2+}, as well as dyes, from the aqueous medium. According to W. Plazinski, polyuronates interact with Mn^{2+} ions by bidentate binding, where the ligand forms two connections with the same core atom or heavy metal

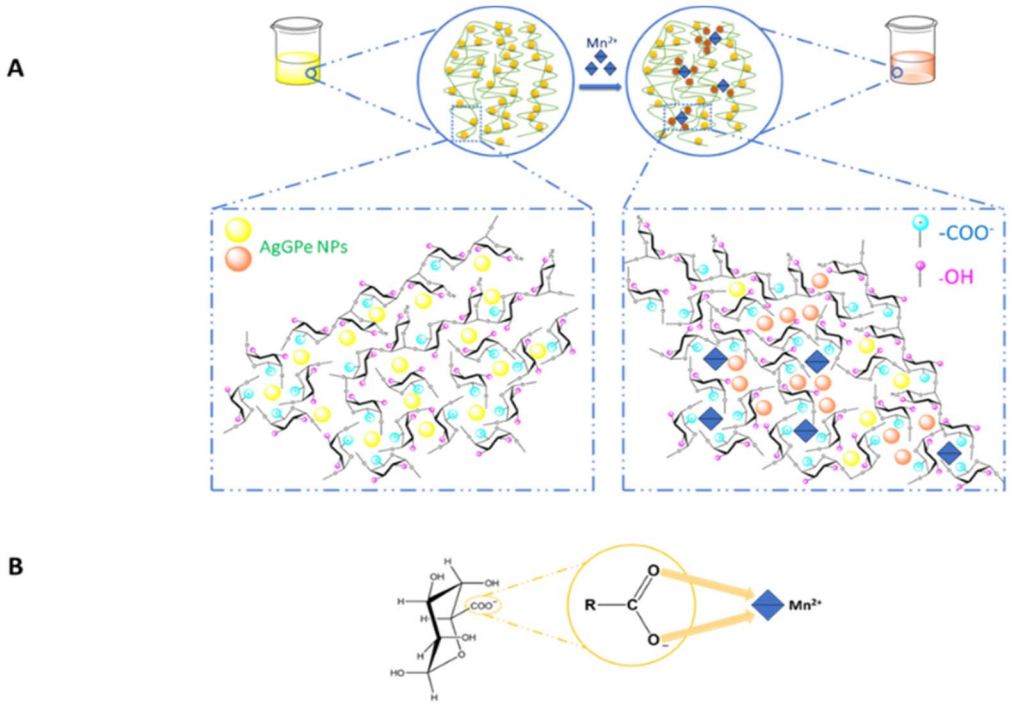

Scheme 3 Schematic of the colorimetric sensing of Mn^{2+} using AgGPe NPs: (A) mechanism, and (B) interaction between the carboxyl group and Mn^{2+} ions.

ion. This result is also observed for Co^{2+} ions, as illustrated in Scheme 3B.

On the other hand, to clarify the color change between nanosilver and Mn^{2+}, an additional experiment was carried out using EDTA 50 mM based on the chelating ability between EDTA and metal cations. In Fig. 4A, AgGPe NPs exhibited the SPR peak at 405 nm (red line); however, after adding Mn^{2+}, the absorbance intensity or wavelength changed (blue line). Nevertheless, by using EDTA before adding Mn^{2+}, the SPR peak of functionalized silver retained its specifications. We can see the change of yellow color of AgGPe NPs (number 1) after adding Mn^{2+} without (number 2) and with EDTA (number 3) in Fig. 4B. This was explained by the ability of EDTA to protect the silver nanoparticles by chelating the manganese(II) ions; thus, we concluded that the color change of AgGPe NPs was induced by binding with Mn^{2+}. The colorimetric detection of AgGPe NPs toward Mn^{2+} occurs owing to the binding of the analyte to the surface ligand and the aggregation of functionalized Ag NPs by inducing a change in the inter-particle distance, which affects the SPR peak, causing a color shift.[3]

Subsequently, we measured the size of the nanosilver particles to assess whether any changes were caused by the presence of Mn^{2+}. It is noteworthy that the sizes of NPs were originally 248.3 ± 91.17 nm, but they increased to 421.4 ± 26.1 nm (data not shown). Additionally, the zeta potential changed from -34.26 mV to −19.50 mV in the presence of Mn^{2+}. Therefore, the Mn^{2+} induced the aggregation of functionalized nanosilver, which is in agreement with the shift in the SPR peak.

3.3. Optimization of sensing parameters

The parameters that influence the binding of the analyte in terms of volume of promoted sensor, incubation time, and pH

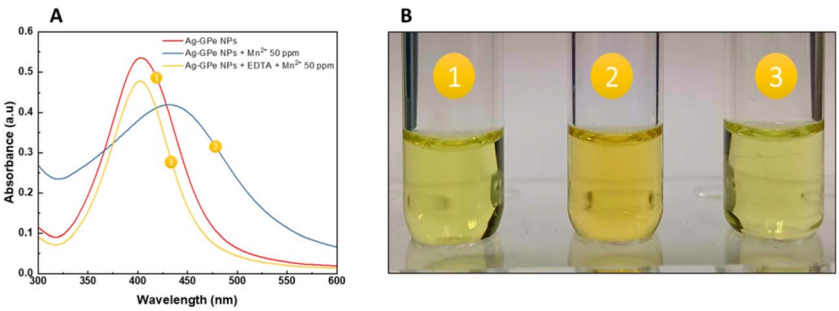

Fig. 4 Effect of EDTA on the detection of manganese ions by grapefruit pectin-decorated silver nanoparticles (AgGPe NPs). (A) UV-vis spectra of AgGPe NPs (sample 1), AgGPe-Mn^{2+} (sample 2), and AgGPe-EDTA-Mn^{2+} (sample 3). (B) Photographs showing the visual appearance of samples 1, 2, and 3.

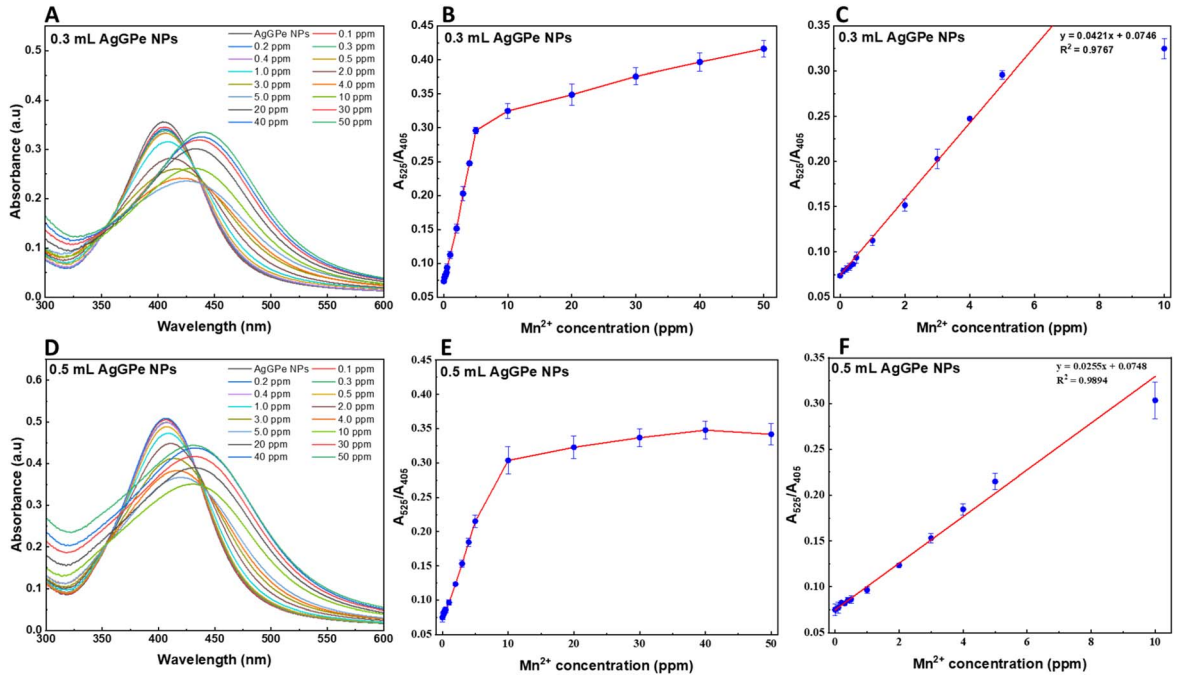

Fig. 5 Effect of AgGPe NP volume on the detection of Mn^{2+} ions. (A–C) UV-vis spectra of 0.3 mL of nanosilver incubated with Mn^{2+} across concentrations ranging from 0 to 50 ppm, the corresponding absorption ratios (A_{525}/A_{405}) as a function of Mn^{2+} concentration, and the linear regression analysis within the 0–10 ppm range, respectively. (D–F) Analogous data obtained using 0.5 mL of nanosilver, including UV-vis spectra, absorption ratio plots, and linear regression analysis.

are indispensable for the feasibility and accuracy of on-site detection; these are depicted in Fig. 5 and 6.

First, the volume of AgGPe NPs was evaluated for easy observation because an insufficient or excessive input of the indicator will result in inaccurate observation by the naked eye. Fig. 5 reflects the optimal input of AgGPe NPs, in which the graphs of A and D show the changes in SPR peaks of silver nanoparticles in the range of 0–50 ppm of Mn^{2+}. However, instead of using 0.3 mL of colorimetric probe, whose absorption ratio was proportional to Mn^{2+} concentration from 0.1–5 ppm, the use of 0.5 mL of AgGPe NPs formed a linear equation up to 10 ppm (Fig. 5B and E). Therefore, 0.5 mL of AgGPe NPs seems to be the optimum amount for sensing, owing to the high correlation coefficient $R^2 = 0.9894$ compared with $R^2 = 0.9767$ by using 0.3 mL (Fig. 5C and F).

Simultaneously, in Fig. 6A, a total of 2 mL solution comprised of 0.5 mL AgGPe NPs with water, and 0.1 mL of Mn^{2+} (0.1–50 ppm) was incubated for determined time intervals. It is easy to conclude that the absorbance ratio A_{525}/A_{405} was proportional to the reaction time and plateaued after 1 hour, which indicates a sufficient timeframe for colorimetric sensing. This requires having enough time for complete contact between the sensor and the analyte. Furthermore, the UV-vis of AgGPe NPs and its complexes, depicted in Fig. 6B, show the shift of the original SPR peaks in accordance with the increase of Mn^{2+} concentration from 0.1 to 50 ppm, from which a linear equation

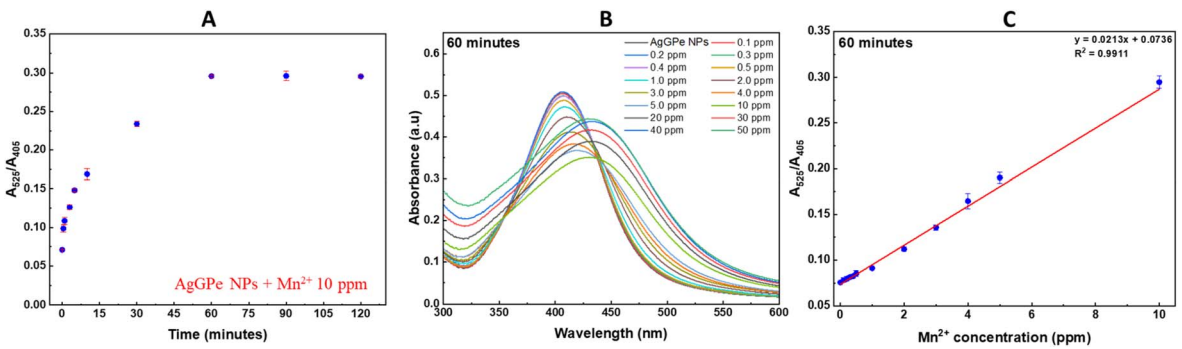

Fig. 6 Effect of incubation time on the detection of Mn^{2+} ions by grapefruit pectin-decorated silver nanoparticles (AgGPe NPs). (A) Relationship between the absorption ratio (A_{525}/A_{405}) and incubation time, (B) variation in the surface plasmon resonance (SPR) of AgGPe NPs at different Mn^{2+} concentrations, and (C) linear regression analysis established within the 0–10 ppm concentration range of Mn^{2+}.

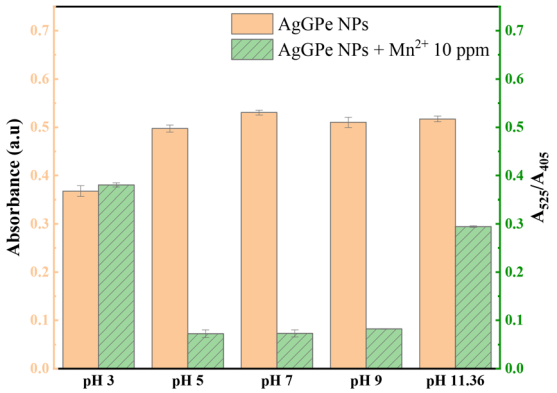

Fig. 7 Evaluation of the sensing performance of grapefruit pectin-decorated silver nanoparticles (AgGPe NPs) at different pH values. The analysis demonstrates how variations in pH influence the optical response and selectivity of AgGPe NPs toward Mn^{2+} ions.

is constructed between the absorbance ratio A_{525}/A_{405} and the Mn^{2+} concentration in range of 0.1–10 ppm with a high correlation coefficient ($R^2 = 0.9911$) (Fig. 6C). Therefore, the subsequent experiment was conducted within one hour to reduce the time of recognition and achieve more reliable results.

To gain general insights into real-life applications, it is essential to assess the sensing ability of AgGPe NPs in various pH environments in accordance with the unpredictable properties of different natural water sources. In Fig. 7, it is shown that the AgGPe NP sensor was stable from pH 5 to 11.36 (post-synthetic conditions), in which the maximum absorbance reached above 0.5 at a wavelength of 405 nm. Specifically, it was strongly reduced at pH 3; thus, the silver nanoparticles were aggregated. In the presence of Mn^{2+}, the sensor exhibited the opposite behavior. Briefly, if the environment was at pH 5–9, the absorption ratios were lowest compared to pH 11.36, which meant that the sensor worked well in this pH range. Meanwhile, pH 3 was not an ideal environment for detecting Mn^{2+} owing to the aggregation of silver nanoparticles. Comparing the results, we discovered that they were comparable to those of the publication by P. Panjina *et al.*,[8] whereby silver nanoparticles were made using *Okara extract* and trisodium citrate (TSC); at pH values between 3 and 9, the silver nanoparticles had a very low capacity to detect Mn^{2+}. Meanwhile, Mn^{2+} sensing worked best in the pH range of 11 to 12. Besides, we believe that the acidic or alkaline environment could influence the negatively charged functional groups at the surface of the silver nanoparticles, the existence of Mn^{2+} oxidative states, and the coordination between ligands and analytes. Therefore, a comprehensive step to evaluate the efficacy of the sensor at different pH values should be conducted in the future to establish an accurate procedure for real water analysis.

3.4. Effect of interferences

It is a pivotal step to evaluate the impact of interference on the sensing ability of nanosilver to simulate real-life activity. Herein, 0.5 mL of nanosilver solution was diluted with 1.3 mL of DD water and subsequently 0.1 mL of competitors (10 ppm for each cation) before adding 0.1 mL of Mn^{2+} (also 10 ppm), we collected the absorbance ratios of A_{525}/A_{405} for comparison with positive and negative controls of AgGPe NPs and AgGPe-Mn^{2+}, respectively; the results are shown in Fig. 8. As we can see, Fig. 8A shows that adding cations such as Cd^{2+}, Co^{2+}, Zn^{2+}, and Ni^{2+} affects the ratio A_{525}/A_{405} compared to the control sample. This is perfectly consistent with the findings of author W. Plazinski *et al.*[28] The grapefruit pectin chains may form complexes with interfering cations due to competition in the complex formation process with carboxylate anions between divalent metals. This reduces the number of complexes between the Mn-pectin polymer chain, resulting in a different recorded signal in comparison to the control sample. Also, the presence of some metal ions that have the same oxidation states or ionic radii can interfere with the binding sites of Mn^{2+} on AgGPe NPs.[3]

On the other hand, using anionic agents as competitors revealed that only thiosulfate ($S_2O_3^{2-}$) can strongly impact the sensing ability, while the other seven anions were negligible (Fig. 8B). This phenomenon for thiosulfate is related to the

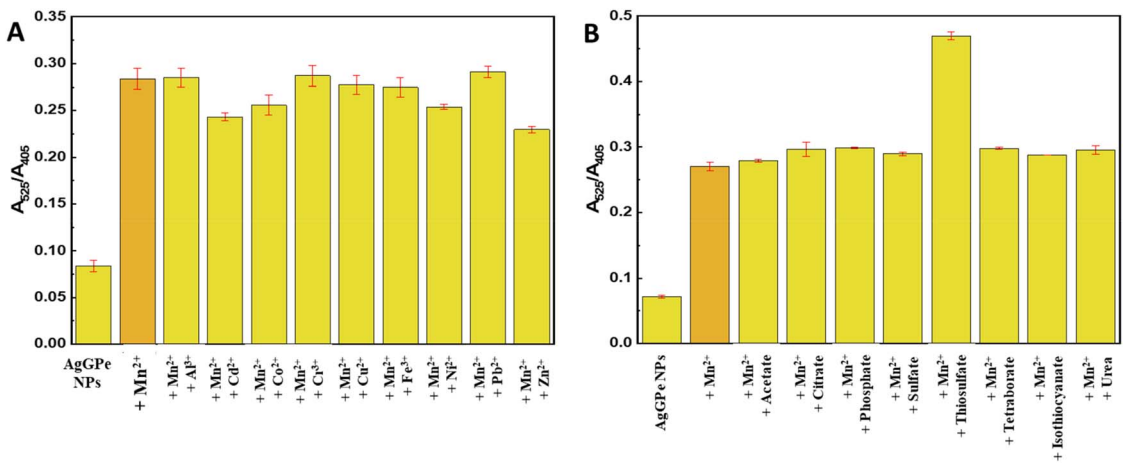

Fig. 8 Analysis of potential interferences in the detection of Mn^{2+} ions using grapefruit pectin-decorated silver nanoparticles (AgGPe NPs). (A) Response of AgGPe NPs (0.5 mL) after incubation with 10 ppm cations for 1 hour, and (B) response of AgGPe NPs (0.5 mL) after incubation with 10 ppm anions for 1 hour.

Table 2 Comparison of our sensor with previously reported AgNP-based sensors

AgNP-based probes	Concentration (ppm)	LOD (ppm)	Ref.
OKR-TSC-AgNPs	0.0250–5.0	0.01	8
L-arginine AgNPs	0–0.0385, 0.2750–3.8500	0.0011	31
Cysteic acid–AgNPs	2.75×10^{-4} – 0.11	2.75×10^{-4}	32
Withania somnifera extract-AgNPs	0.55–11	—	3
Alginate – AgNPs	0.055–0.55	—	4
Lignin-functionalized silver nanoparticles	0.165–4.455, 5.335–8.910	0.0033	7
$(TMB)_2$-PEI/AgNPs (3,3′,5,5′-tetramethylbenzidine (TMB) and polyetherimide (PEI))	0.0011–0.055	0.000055 and 0.011	33
4-MBA-MA-AgNPs (4-mercaptobenzoic acid (4-MBA) and melamine (MA))	0.0275–0.55	0.00275	27
Clove-AgNPs	0.022–0.11	0.011	34
$P_3O_{10}^{5-}$-AgNPs	0.00275–1.1	0.0055	35
$Na_4P_2O_7$-HPMC-AgNPs	0.649–0.6985	0.0275	36
L-tyrosine – AgNPs	0.00088–0.0275	0.00088	9
AgGPe NPs	0.1–10	0.5065	This work

Table 3 Concentration and recovery analysis of Mn^{2+} ions in real water samples using grapefruit pectin-decorated silver nanoparticles (AgGPe NPs)

Samples	Added Mn^{2+} (ppm)	Found Mn^{2+} (ppm) (mean ± SD, $n = 3$)	Recovery (%)	RSD (%)
Drinking water	1	0.9684 ± 0.0135	96.84	1.40
	5	5.0625 ± 0.0593	101.25	1.17
	10	10.2780 ± 0.6199	102.78	6.03
Tap water	1	0.9581 ± 0.0126	95.81	1.31
	5	4.8217 ± 0.0939	96.43	1.95
	10	10.0162 ± 0.4728	100.16	4.72
Tau Hu canal water	1	1.0869 ± 0.0584	108.69	5.38
	5	5.3244 ± 0.0386	106.49	0.73
	10	10.2271 ± 0.5174	102.27	5.06

etching reaction of sodium thiosulfate on the surface of silver nanoparticles to form $[Ag(S_2O_3^{2-})_2]^{3-}$, according to the following reaction:[29,30]

We simultaneously investigated the influence of cations and anions on Mn^{2+} ion sensing to enhance the sensor's practical application. This evaluation demonstrates the sensor's selectivity and robustness against competing ionic species.

Finally, our promoted sensor was compared with other research to assess the potential applications; the results are listed in Table 2. Our work gave a higher LOD compared to other groups. This can be due to the coordination between Mn^{2+} and pectin, which depends on the ratios between pectin and Mn^{2+}, the concentration of pectin, and the manganese valences. In this study, we hypothesize that the concentration of pectin is the core factor resulting in the high LOD. This is attributed to the high viscosity of excessive pectin, which may hinder the movement of AgGPe NPs to come closer in the presence of Mn^{2+}.

3.5. Real sample analysis

AgGPe NPs showed good specific recognition and high sensitivity to Mn^{2+}, thus they were applied to detect the presence of Mn^{2+} in real water sources, such as drinking water, tap water, and Tau Hu canal water, by spiking 1, 5, and 10 ppm of Mn^{2+}; the data are presented in Table 3. Analysis of the drinking water, tap water, and Tau Hu canal water achieved a recovery of 96.84–102.78%, 95.81–100.06%, and 108.69–102.27%, respectively, with the RSD of most samples being less than 6.0%. This data proved the feasibility of AgGPe NPs to sense the introduction of Mn^{2+} in real water.

4. Conclusions

The use of grapefruit pectin as a benign reducing and stabilizing agent explicitly promoted a facile and green method for silver nanoparticle synthesis. The process was influenced by parameters such as the input of pectin and silver nitrate, as well as the pH of the reaction environment, and produced the nanosilver with sizes of 5–45 nm with related physicochemical specifications. The particles were characterized by UV-vis, FTIR, size and zeta potential analysis, XRD, and HR-TEM techniques. They were used as a sensitive, selective, and accurate marker for manganese ions in water, wherein a colorimetric change from yellow to brown could be seen by the naked eye. The linearity was recorded from 0.1 to 10 ppm, with the LOD found to be 0.5065 ppm. Finally, the promoted sensor had good recovery in drinking water, tap water, and canal water tests. We anticipate that pectin-decorated silver nanoparticles are an ideal candidate for many applications.

Author contributions

Khoa Anh Ton and Khang Nguyen-Duy Dao (equal contributions): conceptualization, investigation, data curation, Formal

analysis, writing – original draft, writing – review and editing. Hoa Son Pham: software. Chi Thi-Kim Huynh: validation, supervision. Thu Thi-Cam Nguyen: writing – original draft. Phuc Hoang Nguyen: investigation. Ty Minh Nguyen: methodology. Dung Thi-Kim Hoang: funding acquisition, writing – review and editing, project administration

Conflicts of interest

There are no conflicts to declare.

Data availability

The data that support the findings of this study are available from the corresponding author upon reasonable request.

Supplementary information (SI) is available. See DOI: https://doi.org/10.1039/d5ra08769d.

Acknowledgements

This research was supported by the Vietnam Academy of Science and Technology through fundamental research project TĐPTCB.01/24-26.

References

1 F. Sudarman, M. Shiddiq, B. Armynah and D. Tahir, Silver nanoparticles (AgNPs) synthesis methods as heavy-metal sensors: a review, *Int. J. Environ. Sci. Technol.*, 2023, **20**(8), 9351–9368.

2 S. Tamilselvan, R. M. Soniya, R. Vasantharaja, M. Kannan, S. Supriya, B. P. Dass Batvari, *et al.*, Silver nanoparticles based spectroscopic sensing of eight metal ions in aqueous solutions, *Environ. Res.*, 2022, **212**, 113585.

3 M. U. Rahman, M. W. Ullah, S. A. Alharbi, S. Alfarraj, M. Ul-Islam, M. Y. Ali, *et al.*, Development of a colorimetric sensor for selective manganese detection using green-synthesized silver nanoparticles from Withania somnifera, *Results Chem.*, 2024, **10**, 101733.

4 K. B. Narayanan and S. S. Han, Colorimetric detection of manganese(II) ions using alginate-stabilized silver nanoparticles, *Res. Chem. Intermed.*, 2017, **43**(10), 5665–5674.

5 D. Wang, W. Geng, Q. Li, G. Li, D. Zhang and H. Zhang, Ultrasonic green synthesis of silver nanoparticles mediated by Pectin: Characterization and evaluation of the cytotoxicity, antioxidant, and colorectal carcinoma properties, *Arab. J. Chem.*, 2022, **15**(2), 103500.

6 V. Amendola, O. M. Bakr and F. Stellacci, A Study of the Surface Plasmon Resonance of Silver Nanoparticles by the Discrete Dipole Approximation Method: Effect of Shape, Size, Structure, and Assembly, *Plasmonics*, 2010, **5**(1), 85–97.

7 S. Sharma, A. Jaiswal and K. N. Uttam, Synthesis of Sensitive and Robust Lignin Capped Silver Nanoparticles for the Determination of Cobalt(II), Chromium(III), and Manganese(II) Ions by Colorimetry and Manganese(II) Ions by Surface-Enhanced Raman Scattering (SERS) in Aqueous Media, *Anal. Lett.*, 2021, **54**(12), 2051–2069.

8 P. Panjina, A. Rawat, R. Seedad and K. Songsrirote, Manganese Detection in Water Samples via Photometrix Colorimetric Analysis on Smartphones, by using Silver Nanoparticles Prepared from Okara Extract, *ChemistrySelect*, 2024, **9**(1), e202302425.

9 M. Annadhasan, T. Muthukumarasamyvel, V. R. Sankar Babu and N. Rajendiran, Green Synthesized Silver and Gold Nanoparticles for Colorimetric Detection of Hg2+, Pb2+, and Mn2+ in Aqueous Medium, *ACS Sustain. Chem. Eng.*, 2014, **2**(4), 887–896.

10 S. Sharma, A. Jaiswal and K. N. Uttam, Colorimetric and Surface Enhanced Raman Scattering (SERS) Detection of Metal Ions in Aqueous Medium Using Sensitive, Robust and Novel Pectin Functionalized Silver Nanoparticles, *Anal. Lett.*, 2020, **53**(15), 2355–2378.

11 S. F. Shange, P. N. Kubheka, T. R. Makhanya, P. S. Mdluli and N. Deenadayalu, Development of a highly selective and sensitive colorimetric detection of manganese(II) ion in environmental water using 3-(4-hydroxy-3-methoxyphenyl)-2,3-dihydropyrazolo [3, 4-*b*] indole-1(4*H*)-carbothioamide modified gold nanoparticles: A CIE L*a*b*/Yxy colour space study, *J. Mol. Liq.*, 2025, **427**, 127447.

12 M. Nemiwal, T. C. Zhang and D. Kumar, Pectin modified metal nanoparticles and their application in property modification of biosensors, *Carbohydr. Polym. Technol. Appl.*, 2021, **2**, 100164.

13 P. C. Tran, T. H. D. Nguyen, T. H. A. Nguyen, T. K. C. Huynh and T. K. D. Hoang, Physicochemical Properties of Gel Beads Synthesized from Agricultural By-Products Pectin, *Chem. Eng. Trans.*, 2024, **113**, 295–300.

14 D. M. Aziz, A. A. M. Amin, S. A. Hassan, H. Özmen, G. K. Incili and Y. Say, One-pot synthesis of quercetin-functionalized silver and copper nanoparticles for enhanced optical, antimicrobial, and computational properties, *Sci. Rep.*, 2025, **15**(1), 26391.

15 H. Yu, J. Yu, L. Li, Y. Zhang, S. Xin, X. Ni, *et al.*, Recent Progress of the Practical Applications of the Platinum Nanoparticle-Based Electrochemistry Biosensors, *Front. Chem.*, 2021, **9**, 677876.

16 M. Shellaiah, N. Thirumalaivasan, K. W. Sun and S.-P. Wu, A pH cooperative strategy for enhanced colorimetric sensing of Cr(III) ions using biocompatible L-glutamic acid stabilized gold nanoparticles, *Microchem. J.*, 2021, **160**, 105754.

17 D. G. Altman and J. M. Bland, Standard deviations and standard errors, *BMJ*, 2005, **331**(7521), 903.

18 T. T. Gan, Y. J. Zhang, N. J. Zhao, X. Xiao, G. F. Yin, S. H. Yu, *et al.*, Hydrothermal synthetic mercaptopropionic acid stabled CdTe quantum dots as fluorescent probes for detection of Ag^{+}, *Spectrochim. Acta, Part A Mol. Biomol. Spectrosc.*, 2012, **99**, 62–68.

19 O. Velgosova, L. Mačák, M. Lisnichuk and P. Varga, Influence of pH and Temperature on the Synthesis and Stability of Biologically Synthesized AgNPs, *Appl. Nanosci.*, 2025, **6**(4), 22.

20 T. T. Y. Nhi, D. T. Thien, T. D. Cong, N. T. Tung, L. T. Thuy, N. T. Thuc, *et al.*, Green synthesis of pectin-silver

nanocomposite: Parameter optimization and physico-chemical characterization, *Vietnam J. Chem.*, 2022, **60**(S1), 66–71.

21 S. A. Ibraheem, E. A. Audu, A. J. Atabat, Mu Jaafar, B. F. Tanimu, J. Y. Yahaya, *et al.*, Pectin-stabilized silver nanoparticles: synthesis, optical and antimicrobial activity against E. Coli, *Inorg. Chem. Commun.*, 2023, **158**, 111500.

22 A. K. B. Ayaz, S. K. P and A. Veerappan, A facile method to prepare fluorescent carbon dots and their application in selective colorimetric sensing of silver ion through the formation of silver nanoparticles, *J. Lumin.*, 2016, **177**, 228–234.

23 K. S. U. Suganya, K. Govindaraju, V. G. Kumar, V. Karthick and K. Parthasarathy, Pectin mediated gold nanoparticles induces apoptosis in mammary adenocarcinoma cell lines, *Int. J. Biol. Macromol.*, 2016, **93**, 1030–1040.

24 H. Park, W. Kim, M. Kim, G. Lee, W. Lee and J. Park, Eco-friendly and enhanced colorimetric detection of aluminum ions using pectin-rich apple extract-based gold nanoparticles, *Spectrochim. Acta, Part A Mol. Biomol. Spectrosc.*, 2021, **245**, 118880.

25 B. K. Mehta, M. Chhajlani and B. D. Shrivastava, Green synthesis of silver nanoparticles and their characterization by XRD, *J. Phys.: Conf. Ser.*, 2017, **836**(1), 012050.

26 P. Prosposito, L. Burratti and I. Venditti, Silver Nanoparticles as Colorimetric Sensors for Water Pollutants, *Chemosensors*, 2020, **8**(2), DOI: 10.3390/chemosensors8020026.

27 Y. Zhou, H. Zhao, C. Li, P. He, W. Peng, L. Yuan, *et al.*, Colorimetric detection of Mn2+ using silver nanoparticles cofunctionalized with 4-mercaptobenzoic acid and melamine as a probe, *Talanta*, 2012, **97**, 331–335.

28 W. Plazinski and M. Drach, Binding of bivalent metal cations by α-l-guluronate: insights from the DFT-MD simulations, *New J. Chem.*, 2015, **39**(5), 3987–3994.

29 I. Rivera, F. Patiño, A. Roca and M. Cruells, Kinetics of metallic silver leaching in the O2–thiosulfate system, *Hydrometallurgy*, 2015, **156**, 63–70.

30 X. Hou, S. Chen, J. Tang, Y. Xiong and Y. Long, Silver nanoplates-based colorimetric iodide recognition and sensing using sodium thiosulfate as a sensitizer, *Anal. Chim. Acta*, 2014, **825**, 57–62.

31 Y. He and X. Zhang, Ultrasensitive colorimetric detection of manganese(II) ions based on anti-aggregation of unmodified silver nanoparticles, *Sensor. Actuator. B Chem.*, 2016, **222**, 320–324.

32 Y.-X. Qi, Z.-b Qu, Q.-X. Wang, M. Zhang and G. Shi, Nanomolar sensitive colorimetric assay for Mn2+ using cysteic acid-capped silver nanoparticles and theoretical investigation of its sensing mechanism, *Anal. Chim. Acta*, 2017, **980**, 65–71.

33 Z. Zhang, C. Shang, W. Zhao, Y. Cao, J. Han, C. Hu, *et al.*, 3,3′,5,5′-Tetramethylbenzidine and polyetherimide decorated silver nanoparticles for colorimetric Mn2+ ions detection in aqueous solution, *Chem. Pap.*, 2022, **76**(11), 7253–7260.

34 P. Joshi, M. Nair and D. Kumar, pH-controlled sensitive and selective detection of Cr(iii) and Mn(ii) by using clove (S. aromaticum) reduced and stabilized silver nanospheres, *Anal. Methods*, 2016, **8**(6), 1359–1366.

35 Y.-X. Gao, J.-W. Xin, Z.-Y. Shen, W. Pan, X. Li and A.-G. Wu, A new rapid colorimetric detection method of Mn2+ based on tripolyphosphate modified silver nanoparticles, *Sensor. Actuator. B Chem.*, 2013, **181**, 288–293.

36 G. Wu, C. Dong, Y. Li, Z. Wang, Y. Gao, Z. Shen, *et al.*, A novel AgNPs-based colorimetric sensor for rapid detection of Cu2+ or Mn2+ via pH control, *RSC Adv.*, 2015, **5**(26), 20595–20602.